Miniaturized Dual-Band Negative Group Delay Circuit Using Dual-Plane Defected Structures

Girdhari Chaudhary, *Member, IEEE*, Yongchae Jeong, *Senior Member, IEEE*, and Jongsik Lim, *Senior Member, IEEE*

***Abstract*—In this letter, a design for a dual-band negative group delay circuit (NGDC) using dual-plane U-shaped defected structures is presented. The center frequency and group delay (GD) time of each band are separately controlled by a defected microstrip structure (DMS) and a defected ground structure (DGS) with resistors connected across the DMS and DGS slots. To verify the design concept, the NGDC is designed, fabricated, and compared with the circuit simulation. To get a wideband bandwidth, two NGDCs with different center frequencies are connected in a cascade design. From the measurements, the GD times of -4.54 ± 0.6 ns and -4.20 ± 0.5 ns are obtained at 3.46–3.58 GHz and 5.10–5.20 GHz, respectively.**

***Index Terms*—Distributed transmission line, dual plane defected structures, dual-band negative group delay circuit (NGDC).**

I. Introduction

In RECENT years, various wireless communication standards, such as wireless local area networks (WLANs), world-wide interoperability for microwave access (WiMax), wideband code division multiple access (WCDMA), long-term evolution (LTE), etc., have been developed throughout the world and more standards will likely emerge in the near future. For this reason, the design of multi-band components is necessary.

A negative group delay (GD) implies time advancement in wave propagation; these interesting characteristics have been applied to various communication systems applications [1]–[3]. Various approaches have been applied to design microwave active/passive negative group delay circuits (NGDCs) [1]–[7]. However, a few studies are focused on the design of dual-band NGDCs [8], [9]. A dual-band NGDC using a composite right/left handed (CRLH) transmission line is presented in [9]. However, it is not possible to independently control the GD time of both bands.

The defected transmission line structures such as the photonic bandgap (PBG) structure, DGS, and DMS can provide attenuation at certain resonant frequencies and are applied successfully to the RF microwave circuits [10], [11]. The attenuation characteristic of the DMS or DGS is also used separately in designing single band NGDC [11], [12]. However, none of the studies have applied dual-plane defected structures (DMS and DGS) simultaneously for designing dual-band NGDCs.

In this letter, the attenuation characteristics of the DMS and DGS are utilized together to design a dual-band NGDC. This work allows for the controllability of the GD time at both bands independently.

Manuscript received March 02, 2014; accepted April 28, 2014. Date of publication June 13, 2014; date of current version August 05, 2014. This work was supported by Basic Science Research Program through the National Research Foundation of Korea (NRF) funded by the Ministry of Education, Science, and Technology (2013006660).

G. Chaudhary and Y. Jeong are with the Division of Electronics Engineering, IT Convergence Research Center, Chonbuk National University, Jeonju, Chollabuk-do, Korea (e-mail: ycjeong@jbnu.ac.kr).

J. Lim is with Soonchunhyang University, Chungcheongnam-do 336-745, Korea.

Color versions of one or more of the figures in this letter are available online at http://ieeexplore.ieee.org.

Digital Object Identifier 10.1109/LMWC.2014.2322445

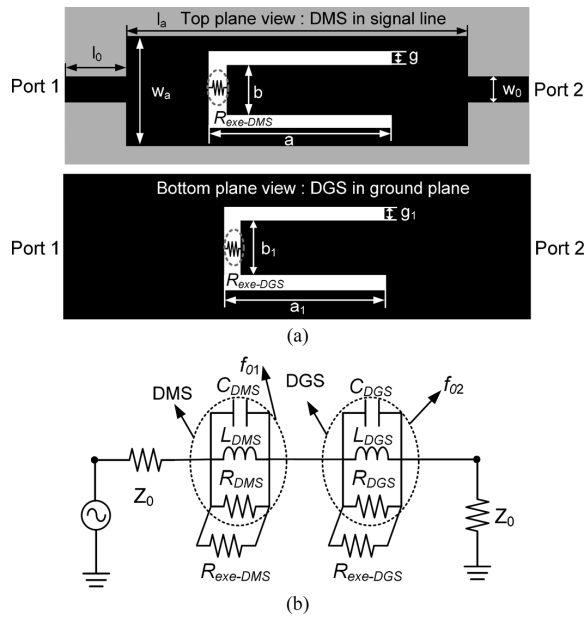

Fig. 1. (a) Proposed structure of dual-band NGDC and (b) its equivalent circuit.

II. Design and Implementation

Fig. 1(a) shows the structure of the proposed dual-band NGDC which consists of a DMS on the top plane and a DGS on the bottom plane. The external resistors are used to get the desired GD times at the center frequencies of the dual-band. The equivalent circuit of the proposed NGDC is shown in Fig. 1(b). The defected structures of the microstrip line such as the DMS and DGS are expressed as a series-parallel RLC circuit. The lumped element values of the equivalent DMS and DGS can be obtained by performing an electromagnetic (EM) simulation whose values are given by [10]. From the equivalent circuit of the proposed structure, the GD and insertion loss can be calculated as shown below [6], [11]

$$\tau\big|_{f=f_{01},f_{02}} = -\frac{1}{2\pi}\frac{d\angle S_{21}}{df} = -\frac{2R_t^2 C_i}{2Z_0+R_t} = -\frac{R_t}{\pi\Delta f_i\left(2Z_0+R_t\right)} \quad (1)$$

$$|S_{21}|_{f=f_{01},f_{02}} = \frac{2Z_0}{2Z_0+R_t}, i = DMS \text{ or } DGS \quad (2)$$

1531-1309 © 2014 IEEE. Personal use is permitted, but republication/redistribution requires IEEE permission.
See http://www.ieee.org/publications_standards/publications/rights/index.html for more information.

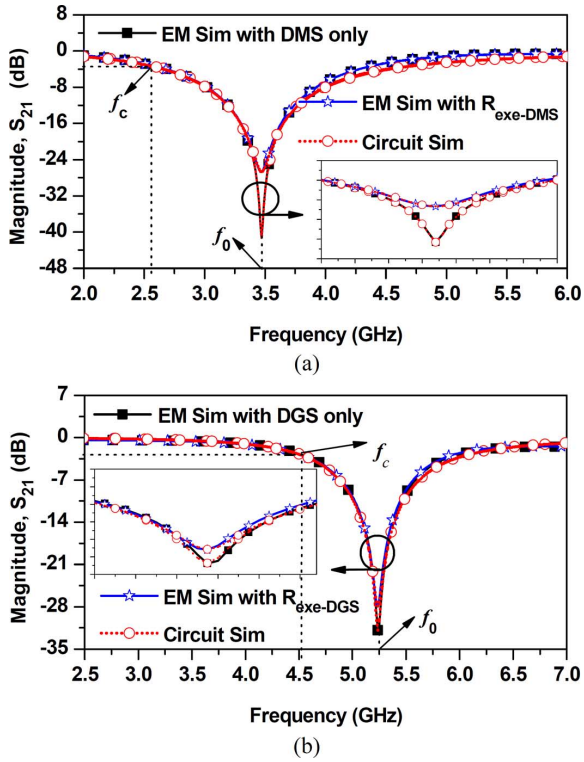

Fig. 2. Electromagnetic and circuit-simulated signal attenuation characteristics of U-shaped DMS and DGS with external resistors: (a) DMS and (b) DGS.

where Z_0 is the termination port impedance. $\Delta f_{\rm i} = 1/2\pi R_{\rm t} C_{\rm i}$ is bandwidth of resonators (DMS and DGS) which is defined as 3 dB frequencies above the maximum signal attenuation for each band. The values of R_t are given as (3)

$$R_t = \frac{R_i R_{exe-i}}{R_i + R_{exe-i}}, i = DMS \text{ or } DGS. \tag{3}$$

From (1) and (3), it is clear that the GD time can be controlled by R_{exe}. To verity the design concept of the proposed NGDC, the U-shaped DMS and DGS are first simulated separately with an EM solver of Ansoft HFSS v13 with the following dimensions: $\rm w_0 = 2.4$, $\rm l_0 = 2$, $\rm w_a = 4$, $\rm a = 15.9$, $\rm b = 2.2$, $\rm g = 0.4$, $\rm a_1 = 10.4$, $\rm b_1 = 2.4$, and $\rm g_1 = 0.4$ (all units are in mm). The simulation is performed using a substrate RT/Duroid 5880 with a dielectric constant $(\varepsilon_{\rm r})$ of 2.2 and thickness (h) of 31 mils.

Fig. 2 shows the simulated characteristics of U-shaped DMS and DGS separately, and that the signal attenuation characteristic can be changed with external resistors. The compact dual-band NGDC can be constructed by utilizing the spaces of the signal and ground planes where the U-shaped DMS and DGS are combined simultaneously on both planes [see Fig. 1(a)].

Fig. 3 shows simulation results of the proposed dual-band NGDC where the dimensions of the U-shaped DMS and DGS are the same as the previous ones. Resonant and cut-off frequencies of first and second band are obtained as $f_{01} = 3.51$ GHz, $f_{02} = 5.21$ GHz, $f_{c_1} = 2.9486$ GHz, and $f_{c_2} = 4.7619$ GHz, respectively. The extracted circuit element values of this structure are given as $C_{DMS} = 1.4024$ pF, $L_{DMS} = 1.4552$ nH, $R_{DMS} = 11.50$ kΩ, $C_{DGS} = 1.6964$ pF, $L_{DGS} = 0.5501$ nH, and $R_{DGS} = 3.83$ kΩ, respectively. In order to get GD of -5 ns, the external resistors at DMS and DGS slots are connected as $R_{exe-DMS} = 2230\ \Omega$ and

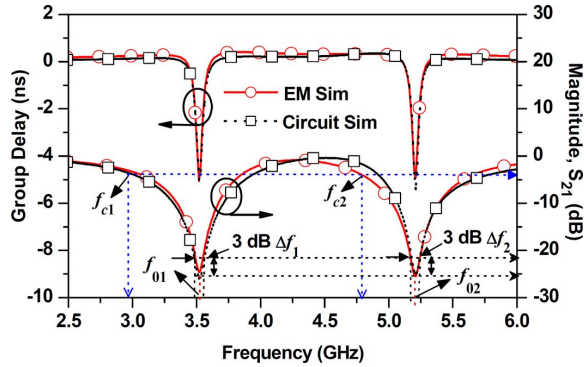

Fig. 3. Simulated group delay and signal attenuation (S_{21}) characteristics of dual-band NGDC.

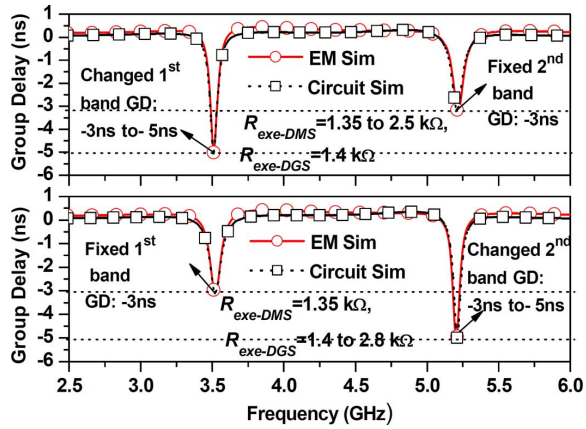

Fig. 4. Simulated group delay characteristics according to different $R_{exe-DMS}$ and $R_{exe-DGS}$.

$R_{exe-DGS} = 2610\ \Omega$, respectively. As seen from the figure, the circuit simulation has good agreement with the EM simulation. The bandwidths of first and second band are determined from the EM simulation as $\Delta f_1 = 58$ MHz and $\Delta f_2 = 60$ MHz, respectively. The GDs at f_{01} and f_{02} are obtained as -4.96 ns and -4.92 ns, respectively. Therefore, maximum achievable NGD time and bandwidth product $(\tau \Delta f_{\rm i})$ of first and second band are given as 0.2876 and 0.2952, respectively.

Fig. 4 shows the simulation results of the GD with different values of external resistors ($R_{exe-DMS}$ and $R_{exe-DGS}$). In order to show independent control of GD, firstly the GD of second band is fixed around -3 ns and the GD of first band is tuned from -3 ns to -5 ns by changing $R_{exe-DMS}$ from 1.35 kΩ to 2.5 kΩ. Similarly, in second case, the first band is fixed at -3 ns and the second band is tuned from -3 ns to -5 ns by changing $R_{exe-DGS}$ from 1.4 kΩ to 2.8 kΩ. However, higher NGD causes the bandwidth decrement. Therefore, it should pay an attention in trade-off between NGD and bandwidth during the design.

III. Simulation and Measurement Results

The goal was to design a GD of -5 ns for WiMax and WLAN operating at a center frequency 3.5 and 5.2 GHz, respectively. For this purpose, a NGDC using the defected structures is simulated and fabricated where the physical dimensions of the U-shaped DMS and DGS are the same as the previous ones.

Fig. 5 shows the simulation and measurement results of the proposed dual-band NGDC. As seen from the figure, the measurement results are in good agreement with the simulation re-

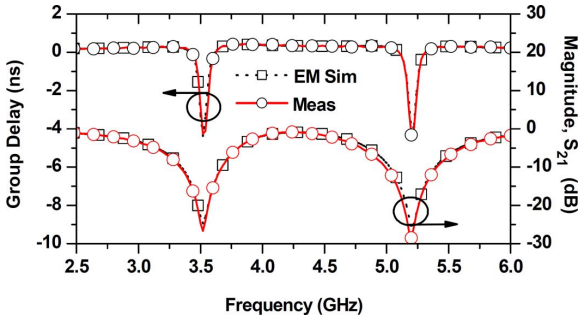

Fig. 5. Simulation and measurement results of single-stage NGDC.

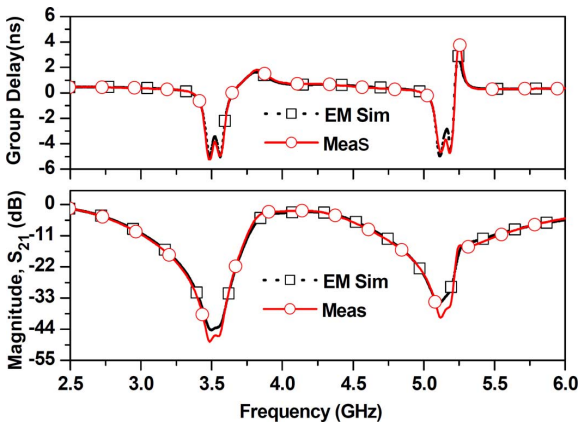

Fig. 6. Simulation and measurement results of two-stage NGDC.

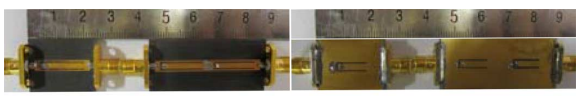

(a) (b)

Fig. 7. Photograph of fabricated dual-band NGDC: (a) top & (b) bottom view.

TABLE I
PERFORMANCE COMPARISON

	Frequencies (GHz)		Circuit Type	NGD (ns)		Out-of-band gain (dB)	NGD x BW product	A
	f_{01}	f_{02}		f_{01}	f_{02}			
[8]	1.05	2.05	Active	-1.16	-0.92	22.5/24.5	0.46/0.55	No
[9]	2.14	3.50	Passive	-3.0	-3.10	34.2/34.9	0.12/0.248	No
This work	**3.50**	**5.15**	**Passive**	**-4.54**	**-4.20**	**47.3/38.8**	**0.545/0.42**	**Yes**

A=Independent control of group delay at each bands

sults. The measured GD and signal attenuation at the first band of 3.516 GHz are -4.24 ns and 26.65 dB, respectively.

Similarly, the GD and signal attenuation at the second band of 5.2 GHz are measured as -4.34 ns and 28.56 dB, respectively. The bandwidths of first and second band are determined as 62 MHz and 59 MHz, which provides the NGD-bandwidth product of 0.2628 and 0.256, respectively. The measured return losses are around 0.3 and 0.4 dB at first and second band center frequencies which can be improved by connecting shunt resistors at input/output ports [6].

To increase the GD bandwidth, the two dual-band NGDCs with slightly different center frequencies are cascaded. For this purpose, two different NGDCs are designed at center frequencies of 3.47 and 3.56 GHz for lower band and 5.11 and 5.19 GHz for higher band, respectively. The measurement results agree well with the simulation results, as shown in Fig. 6. From the measurements, the GDs of -4.54 ± 0.6 ns and -4.20 ± 0.5 ns are obtained at 3.46–3.58 GHz and 5.10–5.20 GHz with NGD-bandwidth products of 0.545 and 0.42, respectively. The signal attenuations at each band are measured as 47.35 ± 0.9 dB and 38.8 ± 0.95 dB, respectively, which can be compensated using general purpose gain amplifier [1], [6]. However, it may decrease overall NGD and increase out-of-band gain and cause stability of overall circuit. The differences in the maximum signal attenuations and the GD at the two center frequencies are observed because the different resistances are used at these frequencies, as extracted inductances of defected structures are different for DMS and DGS.

Table I shows the performance comparison of the proposed circuit with the previous research results. As seen in the table, the proposed dual-band NGDC provides a higher GD with an independently GD control at two bands. However, trade-off between GD and bandwidth is required. The photograph of fabricated circuit is shown in Fig. 7.

IV. CONCLUSION

In this letter, a design and implementation of a dual-band NGDC is presented utilizing the attenuation characteristics of defected microstrip structure and defected ground structure. The proposed structure has greater freedom in controlling the group delay of each band independently. The proposed structure is expected to be applicable for multi-band communication systems.

REFERENCES

[1] H. Choi, Y. Jeong, C. D. Kim, and J. S. Kenney, "Efficiency enhancement of feedforward amplifiers by employing a negative group delay circuit," *IEEE Trans. Microw. Theory Tech.*, vol. 58, no. 5, pp. 1116–1125, May 2010.

[2] B. Ravelo, M. L. Roy, and A. Perennec, "Application of negative group delay active circuits to the design of broadband and constant phase shifters," *Microw. Opt. Tech. Lett.*, vol. 50, no. 12, pp. 3078–3080, Dec. 2008.

[3] C. D. Broomfield and J. K. A. Everand, "Broadband negative group delay circuits for compensation of microwave oscillators and filters," *Electron. Lett.*, vol. 36, no. 23, pp. 1931–1932, Nov. 2003.

[4] B. Ravelo, A. Perennec, M. L. Roy, and Y. G. Boucher, "Active microwave circuit with negative group delay," *IEEE Microw. Wireless Compon. Lett.*, vol. 17, no. 12, pp. 861–863, Dec. 2007.

[5] M. Kandic and G. E. Bridges, "Bilateral gain-compensated negative group delay circuit," *IEEE Microw. Wireless Compon. Lett.*, vol. 21, no. 6, pp. 308–310, Jun. 2011.

[6] M. Kandic and G. E. Bridges, "Asymptotic limits of negative group delay in active resonator based distributed circuits," *IEEE Trans. Circuit Syst. I*, vol. 58, no. 8, pp. 1727–1735, Aug. 2011.

[7] S. Lucyszyn and I. D. Robertson, "Analog reflection topology building blocks for adaptive microwave signal processing applications," *IEEE Microw. Theory Tech.*, vol. 43, no. 3, pp. 601–611, Mar. 1995.

[8] B. Ravelo and S. Blasi, "An FET-based microwave active circuit with dual-band negative group delay," *J. Microw. Optoelectron. Electromagn. Appl.*, vol. 10, no. 2, pp. 355–366, Dec. 2011.

[9] H. Choi, Y. Jeong, J. Lim, S. Eom, and Y. Jung, "A novel design of a dual-band negative group delay circuit," *IEEE Microw. Wireless Compon. Lett.*, vol. 21, no. 1, pp. 19–21, Jan. 2011.

[10] D. Ahn, J. Park, C. Kim, J. Kim, Y. Qian, and T. Itoh, "A design of the low-pass filter using a novel microtrip defected ground structure," *IEEE Trans. Microw. Theory Tech.*, vol. 49, no. 1, pp. 86–93, Jan. 2001.

[11] G. Chaudhary, Y. Jeong, and J. Lim, "Miniaturized negative group delay circuit using defected microstrip structures and lumped elements," *IEEE Int. Microw. Symp. Dig.*, Jun. 2013.

[12] G. Chaudhary, J. Jeong, P. Kim, Y. Jeong, and J. Lim, "Compact negative group delay circuit using defected ground structure," in *Proc. Asia-Pacific Microw. Conf.*, Nov. 2013, pp. 22–24.